Vol. **105** (2004) *ACTA PHYSICA POLONICA A* No. 5

Gd^{3+}–RE^{3+} Exchange Interactions in Rare-Earth Fluoride Crystals (RE = Ce, Nd, Yb)

M.L. Paradowski* and L.E. Misiak

Institute of Physics, Marie Curie-Skłodowska University
Pl. M. Curie-Skłodowskiej 1, 20-031 Lublin, Poland

(Received February 9, 2004)

The investigation of Gd^{3+}-doped LaF_3, $La_{0.9}Ce_{0.1}F_3$, CeF_3, $La_{0.9}Nd_{0.1}F_3$, $LiYF_4$, and $LiY_{0.9}Yb_{0.1}F_4$ single crystals at 4.2 K was carried out in order to study the Gd^{3+}–RE^{3+} exchange interactions (RE = Ce, Nd, Yb). The exchange interactions were estimated by the application of the molecular-field model at liquid-helium temperature, using the g shift from the isostructural diamagnetic hosts LaF_3 and $LiYF_4$ to the paramagnetic hosts. The lattice dynamics is studied by analysing spin-Hamiltonian parameters in the light of the superposition model and the rotational invariance theory for phonon-induced contributions to spin-Hamiltonian parameters. It is suggested from the rotational invariance mechanism for phonon-induced contributions to spin-Hamiltonian parameters that the rotational contributions influence the exchange interactions significantly. Further, the distortions caused by the La^{3+}/Ce^{3+}, La^{3+}/Nd^{3+}, and Y^{3+}/Yb^{3+} substitutions affect significantly the $4f^7$ electron–phonon interactions, as well as the exchange interactions. The magnitude of the isotropic exchange interactions is larger for more symmetrical charge distribution of the $4f^7$ shell.

PACS numbers: 63.20.Kr, 75.30.Et, 75.30.Hx, 76.30.Kg

1. Introduction

In our recent paper [1] the successful way was shown to study the lattice dynamics (from ligands) using the electron paramagnetic resonance (EPR) tech-

---

*corresponding author; e-mail: mlpar@tytan.umcs.lublin.pl nique as well as the superposition model and the rotational invariance theory for phonon-induced contributions to spin-Hamiltonian parameters (SHP). The X-band ($\approx$ 9.5 GHz) EPR studies of Gd^{3+}-doped $\mathrm{LaF_3}$, $\mathrm{La_{0.9}Ce_{0.1}F_3}$, $\mathrm{La_{0.9}Nd_{0.1}F_3}$, $\mathrm{LiYF_4}$, and $\mathrm{LiY_{0.9}Yb_{0.1}F_4}$ single crystals, in the temperature range 4.2–295 K, were carried out in order to investigate the Gd^{3+} spin–phonon interactions [1]. We concluded that the $4f^7$ electron–phonon interactions are strongly dependent on the local structure deformation of the site symmetry of Gd^{3+} ion. Although the variation of the distortion of the local site symmetry is small, it has a strong effect on the constant K_2, which describes the coupling between $4f^7$ electrons and whole phonon spectrum of the crystal lattice. The determined lattice dynamics parameters η (describing the strength of the dynamical part of the crystal field) and $\mathcal{R}_\mathrm{D}$ (describing the ratio of the anharmonic contributions from the rotation to contributions from the strain) also influence significantly the constant K_2 in the investigated crystals. Furthermore, the values of $\mathcal{R}_\mathrm{D}$ in these crystals show that the rotational contributions to the Gd^{3+} SHP from phonons are much smaller than those from the strain.

The purpose of the present paper is to study the effect of the crystal field distortion and the lattice dynamics on the exchange interactions between Gd^{3+} and RE^{3+} (RE = Ce, Nd, Yb) at liquid-helium temperature. We used the EPR technique and the superposition model, because they are very sensitive to the distortion of the crystal lattice. We have chosen the Gd^{3+}-doped $\mathrm{LaF_3}$, $\mathrm{La_{0.9}Ce_{0.1}F_3}$, $La_{0.9}\mathrm{Nd_{0.1}F_3}$, $\mathrm{LiYF_4}$, and $\mathrm{LiY_{0.9}Yb_{0.1}F_4}$ single crystals to compare how different crystal field symmetries can change the spin–phonon interactions. In addition, we used SHP for $\mathrm{CeF_3}$ single crystal from Ref. [2]. We have adopted the theory of the rotational invariance for phonon-induced contributions to SHP developed by Bates and Szymczak [3, 4] which gives more precise description of the observed contribution to SHP from lattice dynamics. The previous results of temperature EPR (X-band) studies in Gd^{3+}-doped $\mathrm{LaF_3}$, $\mathrm{La_{0.9}Ce_{0.1}F_3}$ (and measured presently in the temperature range 4.2–50 K), $\mathrm{La_{0.9}Nd_{0.1}F_3}$, $\mathrm{LiYF_4}$, and $\mathrm{LiY_{0.9}Yb_{0.1}F_4}$ single crystals have been used to investigate the influence of structural and crystal field effects, as well as lattice dynamics (from ligands) on the exchange interactions between the impurity and the host paramagnetic ions. The above samples are the crystals for which well-resolved EPR spectra can be recorded down to liquid-helium temperature.

2. Results and discussion

The crystal growth and crystal structure have been given in Refs. [1, 5–9]. The experimental arrangement has been described elsewhere [9]. The angular variation for Gd^{3+}-doped $\mathrm{LaF_3}$, $\mathrm{La_{0.9}Ce_{0.1}F_3}$, $\mathrm{La_{0.9}Nd_{0.1}F_3}$, $\mathrm{LiYF_4}$, and $\mathrm{LiY_{0.9}Yb_{0.1}F_4}$ single crystals in the ZX plane was shown in Refs. [9–12]. EPR spectra are consistent with the rhombic C_{2v} site symmetry for the Gd^{3+} ion in the D_{3d}^4 trigonal symmetry of lanthanum fluorides, and the tetragonal D_{2d} site symmetry of lithium-yttrium fluorides. The determined g-factors of Gd^{3+} for the $\boldsymbol{Z}$ and $\boldsymbol{X}$ directions in the above single crystals at liquid-helium temperature were used in order to estimate the isotropic exchange interaction.

The average Gd^{3+}–RE^{3+} pair exchange-interaction constant J_p ($\mathcal{H}_p = J_p \boldsymbol{S} \cdot \boldsymbol{S}_1$) is estimated for the paramagnetic host $La_{0.9}Ce_{0.1}F_3$, CeF_3, $La_{0.9}Nd_{0.1}F_3$, and $LiY_{0.9}Yb_{0.1}F_4$ using the molecular-field model [9, 13, 14]. In the Hamiltonian of pair-exchange interaction $\mathcal{H}_p$ the symbols $\boldsymbol{S}$ and $\boldsymbol{S}_1$ are the spin operator of Gd^{3+} ion ($S = \frac{7}{2}$) and the effective spin operator of host ions, respectively. From this model, the total exchange interactions J between Gd^{3+} and its nearest and/or next-nearest paramagnetic RE^{3+} neighbours can be expressed as follows [9, 13, 14]:

$$J = zJ_p = 2(g_{zz}^p - g_{zz}^d)\mu_B B/(P_2 - P_1), \tag{1}$$

where z is the number of nearest and/or next-nearest neighbours paramagnetic RE^{3+} ions surrounding Gd^{3+} dopant ion in the investigated single crystals, the remaining ions are the diamagnetic La^{3+} or Y^{3+} ions, giving no contributions to exchange interactions (it is noted that $z = 12$ for Gd^{3+}-doped CeF_3, NdF_3, and $z = 8$ for $LiYbF_4$, whereas $z = 1$ for Gd^{3+}-doped $La_{0.9}Ce_{0.1}F_3$, $La_{0.9}Nd_{0.1}F_3$, and $LiY_{0.9}Yb_{0.1}F_4$ [6, 9]). The g_{zz}^p and g_{zz}^d are the g-tensor values of Gd^{3+} ion in the isostructural paramagnetic ($La_{0.9}Ce_{0.1}F_3$, CeF_3, $La_{0.9}Nd_{0.1}F_3$, $LiY_{0.9}Yb_{0.1}F_4$) and the diamagnetic (LaF_3, $LiYF_4$) hosts in the $\boldsymbol{Z}$ direction, respectively. Furthermore, μ_B is the Bohr magneton, B (= 340 mT) is the average magnetic field for X-band EPR of Gd^{3+}, P_1 and P_2 are the probabilities of occupation of the two lowest levels in the $^2F_{5/2}$, $^4I_{9/2}$, and $^2F_{7/2}$ ground terms of Ce^{3+}, Nd^{3+}, and Yb^{3+} host ions, respectively. These ground terms split in the presence of the rhombic and tetragonal crystalline electric fields into three, five, and four Kramer's doublets, respectively. However, at liquid-helium temperature only the lowest ground-state doublet is expected to be populated and consequently the effective spin of the host ions is $S_1 = \frac{1}{2}$.

Assuming the Boltzmann distribution, the probabilities are

$$P_i = \exp(-E_i/kT)/\sum_{i=1}^{2}\exp(-E_i/kT), \tag{2}$$

where E_1 and E_2 are energies of the lowest ground-state doublet of RE^{3+} ion and k is Boltzmann's constant.

The energies E_1 and E_2 can be expressed as follows:

$$E_1 = -g_{1z}\mu_B B/2, \tag{3}$$

$$E_2 = g_{1z}\mu_B B/2, \tag{4}$$

where g_{1z} is effective g-factor in the $\boldsymbol{Z}$ direction of RE^{3+} host ion.

The values of g-shifts $\Delta g_{zz} = g_{zz}^p - g_{zz}^d$ and $\Delta g_{xx} = g_{xx}^p - g_{xx}^d$ determined on the basis of the g values in the paramagnetic and diamagnetic hosts are given in Table I (it is noted that $g^d_{zz} = g^d_{xx} = 1.976$ for Gd^{3+}-doped LaF_3 [15] and $g^d_{zz} = 1.9900$, $g^d_{xx} = 1.9897$ for Gd^{3+}-doped LiYF_4 [9]). The results are presented in Table I. The values of g-shifts and effective g-factor for $\mathrm{La}_{0.9}\mathrm{Ce}_{0.1}\mathrm{F}_3$ were determined in this paper using the results of EPR and magnetic susceptibility measurements, respectively. The g_{1z} and g_{1x} values were extrapolated from the formula (4) given in Ref. [16] using the linear scaling of magnetic susceptibility with the mole fraction x of the diamagnetic La ions [17]. (In this purpose, the upper limit of the susceptibility for the $\boldsymbol{X}$ direction was determined for CeF_3 in the powder [18] and in the single crystal along the c axis [19] and a axis [16].) There is a good agreement of the value $g_{1x} = 0.881$ with those equal to 0.90 ± 0.02 for 1% Ce^{3+} in LaF_3 measured at 20 K by Baker and Rubins [20]. Further, using the values of effective g-factor g_{1z} and g_{1x} for the $\boldsymbol{Z}$ and $\boldsymbol{X}$ directions, respectively, the calculations from Eqs. (1)–(4) give the average values of $\mathrm{Gd}^{3+}-\mathrm{RE}^{3+}$ pair exchange-interaction constants J_p. The plot of absolute value of $\mathrm{Gd}^{3+}-\mathrm{RE}^{3+}$ pair exchange-interaction constant J_p versus average distance R_av between the Gd^{3+} and RE^{3+} ions is given in Fig. 1. It can be seen that this dependence is different than those $J_\mathrm{p} \sim \mathrm{e}^{-3.55R}$ or $J_\mathrm{p} \sim R^{-12}$ as reported by Misra and Kahrizi [14].

TABLE I

Values of the Gd^{3+}–RE^{3+} pair exchange-interaction constant J_p in the investigated crystals at liquid-helium temperature are determined from Eqs. (1)–(4). Values of g-factors and g-shifts $\Delta g_{zz} = g^p_{zz} - g^d_{zz}$ and $\Delta g_{xx} = g^p_{xx} - g^d_{xx}$ for Gd^{3+}-doped crystals, as well as values of the effective g-factor g_{1z} and g_{1x} for the host paramagnetic ions for the $\boldsymbol{Z}$ and $\boldsymbol{X}$ directions, respectively, are also included.

Crystal	$\mathrm{La}_{0.9}\mathrm{Ce}_{0.1}\mathrm{F}_3$	CeF_3	$\mathrm{La}_{0.9}\mathrm{Nd}_{0.1}\mathrm{F}_3$	$\mathrm{LiY}_{0.9}\mathrm{Yb}_{0.1}\mathrm{F}_3$
g^p_{zz}	1.9842(3)	2.054(1)[a]	1.9629(5)[c]	1.9661(15)[f]
g^p_{xx}	1.9812(3)	–	1.9993(8)[c]	1.9757(25)[f]
Δg_{zz}	0.0082(3)	0.078(1)	−0.0131(5)	−0.0239(15)[f]
Δg_{xx}	0.0052(3)	–	0.0233(8)	−0.0140(25)[f]
g_{1z}	0.7056	1.03[b]	2.40[d]	1.3308[g]
g_{1x}	0.8810	–	1.092[e]	3.917[g]
J_p [GHz]	−3.07(0.14)	−2.21(0.34)	−2.78(0.16)	3.8(0.3)[f]

[a] Ref. [2], [b] Ref. [16], [c] Ref. [11], [d] Ref. [21], [e] Ref. [20], [f] Ref. [9], [g] Ref. [22]

It is expected that the exchange paths between Gd^{3+} and RE^{3+} ions take place via the intermediary of $2s$ and $2p$ orbitals of ligand F^- ions in the investigated crystals. Therefore, it is very important to analyse the influence of a distortion of the crystalline electric field in the surroundings of the Gd^{3+} ion and lattice dynamics from ligands on the exchange interactions between Gd^{3+} and RE^{3+} ions at liquid-helium temperature. In this purpose we adopted the superposition model [23, 24] and the rotational invariance theory for phonon-induced contributions to

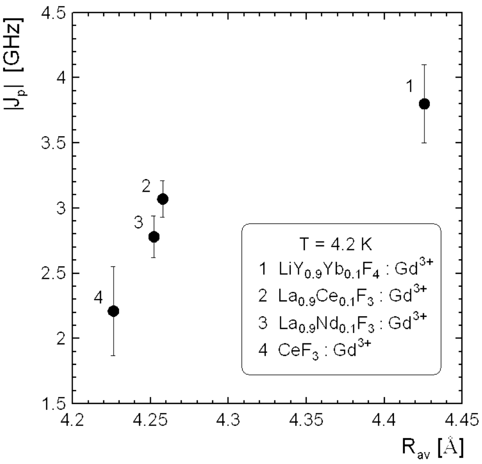

Fig. 1. The absolute value of $Gd^{3+}-RE^{3+}$ pair exchange-interactions constant J_p as a function of the average distance R_{av} between Gd^{3+} and RE^{3+} ions in the investigated crystals.

SHP [1, 3, 4]. The rigid-lattice value $\bar{b}_2(\mathrm{RL})$ of the intrinsic parameter $\bar{b}_2$ (i.e. the value of $\bar{b}_2$ at $T = 0$ K minus zero point vibrations), for Gd^{3+}-doped all investigated crystals, was taken from Table in Ref. [1]. Further, the value of the intrinsic parameter $\bar{b}_2$ for Gd^{3+}-doped CeF_3 single crystal was evaluated from the superposition model using the values of b_2^0 and b_2^2 from Ref. [2]. These values at 4.2 K were determined by extrapolation of the square function [7, 9, 11, 12]. We have determined $b_2^0 = 0.5956 \pm 0.0200$ GHz and $b_2^2 = -0.01 \pm 0.05$ GHz at 4.2 K for Gd^{3+}-doped CeF_3. Finally, using the above results and the superposition model, we have received $\bar{b}_2 = -3.6216 \pm 0.0300$ GHz. The $\bar{b}_2(\mathrm{RL})$ was determined using the fitting of $\bar{b}_2$ to temperature T in the range 200–373 K from the following equation [1]:

$$\bar{b}_2(T) = \bar{b}_2(\mathrm{RL}) + K_2\left(1 + 8\frac{T^4}{\theta_\mathrm{D}^4}\int_0^{\theta_\mathrm{D}/T}\frac{x^3}{\mathrm{e}^x - 1}\mathrm{d}x\right), \tag{5}$$

where K_2 is the coupling constant describing the magnitude of Gd^{3+} spin–phonon interaction and θ_D is the Debye temperature ($\theta_\mathrm{D} = 397$ K for CeF_3 [25]). We have determined, for example, that parameter $\bar{b}_2(\mathrm{RL}) = -4.5202 \pm 0.0300$ GHz for Gd^{3+}-doped CeF_3.

The anharmonic contribution from the strain δD to the SHP D $(= b_2^0)$ is given by the relation [1]:

$$\delta D = p[\bar{b}_2(T) - \bar{b}_2(\mathrm{RL})], \tag{6}$$

where $p = 0.67$ for $La_xRE_{1-x}F_3$ and $p = 0.78$ for $LiY_{1-x}Yb_xF_4$ in the investigated temperature range 4.2–295 K.

Further, the anharmonic contributions from the strain δD and from the rotation δD_{r} to D are given by the equations [4]:

$$\delta D=\frac{-\hbar}{32\pi^2\rho}\left(G_{11}+G_{12}+G_{13}\right)\left(v_{\mathrm{l}}^{-5}+2v_{\mathrm{t}}^{-5}\right)f\left(\omega_{\mathrm{D}},T\right), \tag{7}$$

and

$$\delta D_{\mathrm{r}}=\frac{-\hbar}{32\pi^2\rho}Dv_{\mathrm{t}}^{-5}f(\omega_{\mathrm{D}},T), \tag{8}$$

where G_{11}, G_{12}, G_{13} are the components of the A_1-type magnetoelastic tensor (fully symmetric deformation), ρ is the density of the crystal, v_{l} and v_{t} are the longitudinal and the transversal velocities of sound, respectively, and

$$f(\omega_{\mathrm{D}},T)=\omega_{\mathrm{D}}^4+8\left(\frac{kT}{\hbar}\right)^4\int_0^{\theta_{\mathrm{D}}/T}\frac{x^3}{\mathrm{e}^x-1}\mathrm{d}x, \tag{9}$$

where $\hbar\omega_{\mathrm{D}}=k\theta_{\mathrm{D}}$.

The values of sound velocities at liquid-helium temperature were calculated using elastic constants from Refs. [26, 27] for the elastic waves polarized in the [100], [010], and [001] directions.

The ratio of the anharmonic contributions from the rotation (δD_{r}) to contributions from the strain (δD) is given by the relation [4]:

$$\mathcal{R}_{\mathrm{D}}=\frac{\delta D_{\mathrm{r}}}{\delta D}. \tag{10}$$

The Gd^{3+} spin–phonon interaction constant K_2 from Eq. (5) can be expressed in terms of the magnetoelastic tensor components as follows [1]:

$$K_2=\frac{-\hbar\omega_{\mathrm{D}}^4\left(v_{\mathrm{l}}^{-5}+2v_{\mathrm{t}}^{-5}\right)}{32p\pi^2\rho}\left(G_{11}+G_{12}+G_{13}\right). \tag{11}$$

The parameter η, describing the strength of the dynamical part of the crystal field, is evaluated from the formula [1]:

$$\eta=\frac{\delta D}{|G|}. \tag{12}$$

On the other hand, the parameter η is defined by the expression [28]:

$$\eta=\frac{\langle u^2\rangle}{R_0^2}, \tag{13}$$

where $\langle u^2\rangle$ is the mean square displacement of ligands from their equilibrium positions, and R_0 is the equilibrium minimal distance between the rare-earth ion and ligands.

The calculations from Eqs. (6)–(10) yield the values of anharmonic contributions from the strain δD and from the rotation δD_{r}, the sum values of magnetoelastic tensor components $G=G_{11}+G_{12}+G_{13}$, and the ratio $\mathcal{R}_{\mathrm{D}}$ (Table II). The results of the ratio $\mathcal{R}_{\mathrm{D}}$ for the investigated samples at liquid-helium temperature are in agreement with those obtained in Ref. [4], using the isotropic continuum

TABLE II

Values of the lattice dynamic parameters K_2, δD, δD_r, G, $|\mathcal{R}_\mathrm{D}|$, η, and u for the Gd^{3+}-doped crystals at liquid-helium temperature are determined from Eqs. (6)–(13). The D is the static b_2^0 parameter, and R_0 is the equilibrium reference distance between Gd^{3+} and F^- ions at liquid-helium temperature. The parameters $\mathcal{R}_\mathrm{D}$ and η are dimensionless.

Crystal	LaF_3	$La_{0.9}Ce_{0.1}F_3$	$La_{0.9}Nd_{0.1}F_3$
K_2 [GHz]	0.5334(200)	0.5284(305)	0.6638(314)
D [GHz]	0.6970(20)	0.6980(33)	0.6523(47)
δD [GHz]	0.3574(134)	0.3540(204)	0.4448(210)
δD_r [GHz] $\times 10^{-5}$	−231.9(0.7)^a	−233.0(1.1)^a	−219.4(1.6)^a
	−210.3(0.6)^b	−211.3(1.0)^b	−198.9(1.4)^b
G [GHz]	−53.39(2.00)^a	−52.70(3.04)^a	−65.73(3.11)^a
	−58.56(2.20)^b	−57.79(3.34)^b	−72.09(3.41)^b
$|\mathcal{R}_\mathrm{D}| \times 10^{-3}$	6.49(0.26)^a	6.58(0.41)^a	4.93(0.27)^a
	5.88(0.24)^b	5.97(0.37)^b	4.47(0.24)^b
$\eta \times 10^{-3}$	6.69(0.50)^a	6.72(0.78)^a	6.77(0.64)^a
	6.10(0.46)^b	6.13(0.71)^b	6.17(0.58)^b
R_0 [Å]	2.4146	2.4127	2.4093
u [Å]	0.1975(74)^a	0.1977(114)^a	0.1982(94)^a
	0.1886(71)^b	0.1888(109)^b	0.1892(90)^b

Crystal	CeF_3	$LiYF_4$	$LiY_{0.9}Yb_{0.1}F_4$
K_2 [GHz]	0.8986(600)	0.1662(164)	0.2043(267)
D [GHz]	0.5956(200)	-2.6002(17)	-2.5644(40)
δD [GHz]	0.6020(402)	0.1297(128)	0.1593(208)
δD_r [GHz] $\times 10^{-5}$	−200.9(6.7)^a	448.9(0.3)^a	421.0(0.7)^a
	−182.3(6.1)^b	449.6(0.3)^b	421.6(0.7)^b
G [GHz]	−88.68(5.92)^a	−36.87(3.65)^a	−47.66(6.23)^a
	−97.18(6.49)^b	−36.21(3.58)^b	−46.81(6.12)^b
$|\mathcal{R}_\mathrm{D}| \times 10^{-3}$	3.34(0.33)^a	34.62(3.45)^a	26.42(3.49)^a
	3.03(0.30)^b	34.68(3.45)^b	26.46(3.50)^b
$\eta \times 10^{-3}$	6.79(0.91)^a	3.52(0.70)^a	3.34(0.87)^a
	6.19(0.83)^b	3.58(0.71)^b	3.40(0.89)^b
R_0 [Å]	2.3959	2.2617	2.2590
u [Å]	0.1974(132)^a	0.1341(133)^a	0.1306(172)^a
	0.1886(126)^b	0.1353(135)^b	0.1318(174)^b

[a] determined for elastic waves polarized in the [001] direction;
[b] determined for elastic waves polarized in the [100] and [010] directions

phonon model for orbital singlet ions in low symmetry crystal field; i.e. the rotational contributions are much smaller than those from the strain. The determined from Eqs. (11)–(13) values of the coupling constant K_2, the parameter η and the amplitude u of ligand vibrations in the investigated samples at liquid-helium temperature are also given in Table II. It can be seen that the values of the dynamical parameters G, $\mathcal{R}_\mathrm{D}$, η, and u determined for the elastic waves polarized in the [001], and [100], [010] directions, differ slightly almost in the range of errors. The differences of the dynamical parameter δD_r in these directions are due to small anisotropy of transversal sound velocity. It confirms correctness of the rotational invariance theory used for the phonon-induced contributions to SHP for orbital singlet ions in low symmetry crystal fields at liquid-helium temperature. Furthermore, the same order of magnitude of amplitude u as in present paper is determined from a model of the transferred hyperfine interactions of ^{19}F ligands with Gd^{3+} in PbF$_2$ and SrF$_2$ [29].

The coupling constant K_2 can be expressed using Eqs. (7), (8), (10), and (11) in the simpler form

$$K_2 = \frac{-\hbar\omega_\mathrm{D}^4 D v_\mathrm{t}^{-5}}{32 p \pi^2 \rho \mathcal{R}_\mathrm{D}}. \tag{14}$$

The Gd^{3+} spin–phonon coupling constant K_2 versus the dynamical parameter $|\mathcal{R}_\mathrm{D}|$ for the investigated Gd^{3+}-doped crystals in the temperature range 4.2–295 K is plotted in Fig. 2. It can be seen that the dependence is stronger in the case of lower distortion of the crystal symmetry. The rhombic C_{2v} site symmetry for the Gd^{3+}

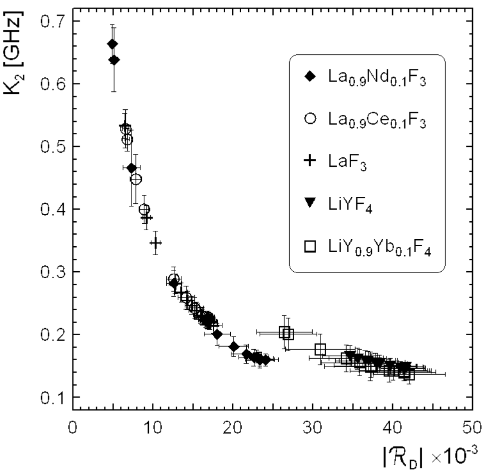

Fig. 2. The $4f^7$ electron–phonon coupling constant K_2 as a function of the absolute value of the ratio $|\mathcal{R}_\mathrm{D}|$ of the anharmonic rotational to the vibrational contributions for elastic waves polarized in the [001] direction for Gd^{3+}-doped investigated crystals in the temperature range 4.2–295 K. The parameter $\mathcal{R}_\mathrm{D}$ is dimensionless.

ion in the D_{3d}^4 trigonal symmetry of lanthanum–(rare-earth) fluorides is lower than the tetragonal D_{2d} site symmetry of lithium–yttrium–(rare-earth) fluorides. This shows that the lowering symmetry of the crystal field changes significantly the $4f^7$ electron–phonon coupling constant K_2. The coupling constant K_2 for Gd^{3+} in $\mathrm{CeF_3}$ is the largest and equal to 0.8986 ± 0.0600 GHz, whereas the absolute value of the dynamical parameter $|\mathcal{R}_\mathrm{D}|$ is the smallest and equal to 3.34 ± 0.33 at 4.2 K (Table II). It can be concluded on the basis of Fig. 2 that the site symmetry of Gd^{3+} in $\mathrm{CeF_3}$ is C_2 at 4.2 K because C_2 is lower than C_{2v}. This conclusion is supported in Ref. [30]. There is a significant effect of the masses difference of composite ions and complexity of the crystal on the dynamical parameter $\mathcal{R}_\mathrm{D}$ (see Table II). The ratio $|\mathcal{R}_\mathrm{D}|$, which describes dynamics, is one order of magnitude larger in lithium–yttrium–(rare-earth) fluorides than in lanthanum–(rare-earth) fluorides.

Below we analyse the influence of the dynamical parameters K_2 and $\mathcal{R}_\mathrm{D}$ on the exchange interactions constant J_p between Gd^{3+} and RE^{3+} ions. We have plotted the relations $|J_\mathrm{p}|$ versus K_2 in Fig. 3 and J_p versus $\mathcal{R}_\mathrm{D}$ in Fig. 4. There are strong linear correlations between the values of these parameters. The coefficients of correlation are equal to 0.9995 and 0.9990 for the plots in Fig. 3 and Fig. 4, respectively. Such strong correlations suggest the existence of a common mechanism responsible for the $4f^7$ electron–phonon and exchange interactions. The mechanism may be related partly to the polarization of ligand F^- ions. The polarizability depends on the surroundings of the F^- ions, and it is larger in $\mathrm{LiYF_4}$ than in $\mathrm{LaF_3}$. The electrostatic polarization of ligands, caused by the distortion of lattice, can produce a large contribution to the $\bar{b}_2$. Further, the distortions caused

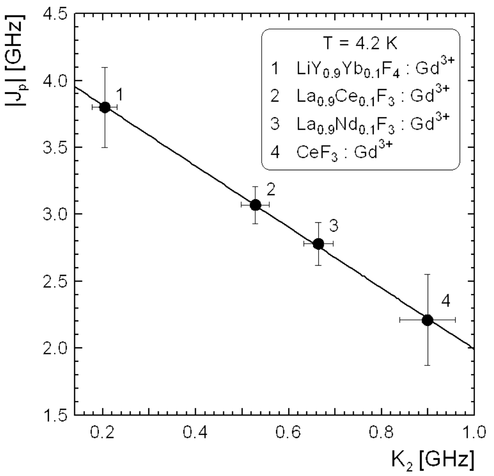

Fig. 3. The absolute value of the exchange interactions constant $|J_\mathrm{p}|$ for Gd^{3+}–RE^{3+} pair in the investigated crystals as a function of the $4f^7$ electron–phonon coupling constant K_2 at liquid-helium temperature.

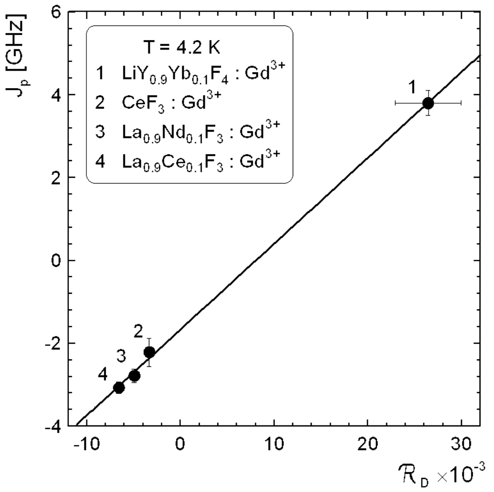

Fig. 4. The exchange interactions constant J_p for Gd^{3+}–RE^{3+} pair as a function of the ratio $\mathcal{R}_\mathrm{D}$ of the anharmonic rotational to the vibrational contributions for elastic waves polarized in the [001] direction for Gd^{3+}-doped investigated crystals at liquid-helium temperature.

by the $\mathrm{La}^{3+}/\mathrm{Ce}^{3+}$, $\mathrm{La}^{3+}/\mathrm{Nd}^{3+}$, and $\mathrm{Y}^{3+}/\mathrm{Yb}^{3+}$ substitutions, affect significantly the $4f^7$ electron–phonon and exchange interactions. The lattice dynamics due to the strain (δD) and due to the rotational-type displacements of the ligand F^- ions (δD_r), as well as the temperature-induced distortion of a Gd^{3+} site symmetry, can change the charge distribution of the $4f^7$ shell. The increase in the temperature-induced distortion of the Gd^{3+} site symmetry and of the K_2 value, causes the decrease in the J_p absolute value (see Fig. 3). On the other hand, the increase in the $\mathcal{R}_\mathrm{D}$ value causes the increase in the J_p value (see Fig. 4). Thus, the larger rotation-type displacements of the F^- ions in $\mathrm{LiY_{0.9}Yb_{0.1}F_4}$ crystals, contrary to $\mathrm{La_{0.9}Ce_{0.1}F_3}$, $\mathrm{La_{0.9}Nd_{0.1}F_3}$, and $\mathrm{CeF_3}$ crystals, cause additional polarization of the $4f^7$ shell. These static and dynamic effects can cause a more spherical distribution of the $4f^7$ electrons in $\mathrm{LiY_{0.9}Yb_{0.1}F_4}$ than in $\mathrm{CeF_3}$. Such mechanism explains stronger isotropic exchange interactions between Gd^{3+} and Yb^{3+} in $\mathrm{LiY_{0.9}Yb_{0.1}F_4}$ than that between Gd^{3+} and Ce^{3+} in $\mathrm{CeF_3}$, as shown in Fig. 1.

Since the lattice dynamics from the ligand F^- ions influence significantly the isotropic exchange interactions of the Gd^{3+}–RE^{3+} ions, it is important to study spin–spin relaxation. The spin–spin relaxation time τ_2, arising from strong dipole–dipole interactions between Gd^{3+} and RE^{3+} ions, can be determined from the equation [31]:

$$\tau \approx \frac{1}{2\pi\Delta\nu}. \tag{15}$$

Using the relation given by Van Vleck [32]:

$$2\Delta\nu = 2.35\sqrt{\langle\Delta\nu^2\rangle_{\rm av}}, \tag{16}$$

the final form is as follows:

$$\tau_2 \approx \frac{1}{2.35\pi\sqrt{\langle\Delta\nu^2\rangle_{\rm av}}}, \tag{17}$$

where $\langle\Delta\nu^2\rangle_{\rm av}$ is the second moment (mean-square power frequency deviation from Larmor frequency ν_0) of the resonance line. According to Van Vleck [32], the second moment can be obtained from the relation (14) in Ref. [11].

The spin–spin relaxation times τ_2, determined from Eqs. (17) are equal to $(6.37 \pm 0.16) \times 10^{-11}$, $(2.65 \pm 0.02) \times 10^{-11}$, $(1.56 \pm 0.05) \times 10^{-11}$, and $(5.48 \pm 0.21) \times 10^{-11}$ s at 4.2 K for Gd^{3+}-doped La$_{0.9}$Ce$_{0.1}$F$_3$, La$_{0.9}$Nd$_{0.1}$F$_3$, CeF$_3$, and LiY$_{0.9}$Yb$_{0.1}$F$_4$, respectively. It can be seen that τ_2 is larger approximately by factor 2 in La$_{0.9}$Ce$_{0.1}$F$_3$ than in La$_{0.9}$Nd$_{0.1}$F$_3$. It is confirmed by the determined spin-bath (liquid-helium) relaxation time $\tau_{\rm b}$ that is one order of magnitude larger in Ce^{3+}(1%)-doped LaF$_3$ than in Nd^{3+}(1%)-doped LaF$_3$ crystal [33]. The smallest value of the spin–spin relaxation time τ_2 was determined in Gd^{3+}-doped CeF$_3$ crystal. Further, in Gd^{3+}-doped LiY$_{0.9}$Yb$_{0.1}$F$_4$ crystal the spin–spin relaxation time τ_2 is close to that in Gd^{3+}-doped La$_{0.9}$Ce$_{0.1}$F$_3$. Thus, the fast spin–spin relaxation can cause weakness of the isotropic exchange interactions ($J_{\rm p}$) between Gd^{3+} and Ce^{3+} in CeF$_3$, as well as that between Gd^{3+} and Nd^{3+} in La$_{0.9}$Nd$_{0.1}$F$_3$. This effect may be related to the mechanism discussed earlier that induces deformation of the charge distribution of the $4f^7$ shell. The sign of the isotropic exchange interactions constant $J_{\rm p}$ can be explained by differences in crystallographic structure of the investigated crystals. The Gd^{3+}–Ce^{3+} pairs in La$_{0.9}$Ce$_{0.1}$F$_3$ and CeF$_3$, and Gd^{3+}–Nd^{3+} pairs in La$_{0.9}$Nd$_{0.1}$F$_3$ have their magnetic moments ordered antiferromagnetically. On the other hand, the Gd^{3+}–Yb^{3+} pairs in LiY$_{0.9}$Yb$_{0.1}$F$_4$ have their magnetic moments ordered ferromagnetically.

3. Conclusions

It is concluded that the Gd^{3+}–RE^{3+} (RE = Ce, Nd, Yb) isotropic exchange interactions are strongly dependent on the local structure deformation of the site symmetry of Gd^{3+} ion. Although the variation of the distortion of the local site symmetry is small, it has a strong effect on the constant $J_{\rm p}$ which describes the isotropic exchange interactions between Gd^{3+} and RE^{3+} ions in the investigated La$_{0.9}$Ce$_{0.1}$F$_3$, La$_{0.9}$Nd$_{0.1}$F$_3$, CeF$_3$, and LiY$_{0.9}$Yb$_{0.1}$F$_4$ single crystals at liquid-helium temperature.

The isotropic exchange interactions constant $J_{\rm p}$ is stronger in LiY$_{0.9}$Yb$_{0.1}$F$_4$ than in CeF$_3$, as well as in La$_{0.9}$Ce$_{0.1}$F$_3$ than in La$_{0.9}$Nd$_{0.1}$F$_3$ due to the smaller temperature-induced distortion of Gd^{3+} site symmetry in LiY$_{0.9}$Yb$_{0.1}$F$_4$, contrary to CeF$_3$, as well as in La$_{0.9}$Ce$_{0.1}$F$_3$, contrary to La$_{0.9}$Nd$_{0.1}$F$_3$. The temperature-induced distortion of the lattice causes the lowering of the symmetry of Gd^{3+} surrounding in Gd^{3+}-doped La$_{0.9}$Ce$_{0.1}$F$_3$, La$_{0.9}$Nd$_{0.1}$F$_3$, and CeF$_3$ crystals at low temperatures. The lattice dynamics parameters K_2 and $\mathcal{R}_{\mathrm{D}}$ caused by the static and dynamic distortions influence significantly the isotropic exchange interactions of Gd^{3+} ($4f^7$) with Ce^{3+} ($4f^1$), or Nd^{3+} ($4f^3$), or Yb^{3+} ($4f^{13}$) ions in the investigated crystals. The dynamic contribution due to the rotation (δD_{r}) causes more symmetrical distribution of the $4f^7$ electrons. On the other hand, the dynamic contribution due to the strain (δD) and the static contributions due to the deformation induced by the substitution of ions, as well as due to the temperature-induced distortion, cause the less symmetrical charge distribution. This effect is reflected in the magnitude of the isotropic exchange interactions that is stronger for more symmetrical charge distribution of the $4f^7$ shell. In this paper we have shown the successful way to study the isotropic exchange interactions in the light of lattice dynamics (from ligands) using the EPR technique and the superposition model, as well as the rotational invariance theory for phonon-induced contributions to SHP from the lattice anharmonicity.

References

[1] M.L. Paradowski, L.E. Misiak, *Acta Phys. Pol. A* **102,** 373 (2002).

[2] S.K. Misra, G. Bacquet, F. Fabre, *Solid State Commun.* **62,** 729 (1987).

[3] C.A. Bates, H. Szymczak, *Phys. Status Solidi B* **74,** 225 (1976).

[4] C.A. Bates, H. Szymczak, *Z. Phys. B* **28,** 67 (1977).

[5] W. Korczak, P. Mikołajczak, *J. Cryst. Growth* **61,** 601 (1983).

[6] M.L. Paradowski, W. Korczak, L.E. Misiak, Z. Korczak, *Proc. SPIE* **3724,** 47 (1999).

[7] M.L. Paradowski, L.E. Misiak, W. Korczak, Z. Korczak, *Proc. SPIE* **4412,** 242 (2001).

[8] L.E. Misiak, P. Mikołajczak, M. Subotowicz, *Phys. Status Solidi A* **97,** 353 (1986).

[9] L.E. Misiak, S.K. Misra, P. Mikołajczak, *Phys. Rev. B* **38,** 8673 (1988).

[10] M.L. Paradowski, L.E. Misiak, *Nukleonika* **42,** 543 (1997).

[11] M.L. Paradowski, L.E. Misiak, *Acta Phys. Pol. A* **95,** 367 (1999).

[12] L.E. Misiak, P. Mikołajczak, *Acta Phys. Pol. A* **75,** 621 (1989).

[13] M.R. St. John, R.J. Myers, *Phys. Rev. B* **13,** 1006 (1976).

[14] S.K. Misra, M. Kahrizi, *Phys. Rev. B* **37,** 5890 (1988).

[15] S.K. Misra, P. Mikołajczak, S. Korczak, *J. Chem. Phys.* **74,** 922 (1981).

[16] M.L. Paradowski, A. Pacyna, A. Bombik, W. Korczak, S.Z. Korczak, *J. Magn. Magn. Mater.* **212,** 381 (2000).

[17] M.L. Paradowski, M. Kulik, W. Korczak, Z. Korczak, *Proc. SPIE* **4412,** 246 (2001).

[18] S. Kern, P.M. Raccah, *J. Phys. Chem. Solids* **26,** 1625 (1965).

[19] C. Leycuras, H. Le Gall, M. Guillot, A. Marchand, *J. Appl. Phys.* **55,** 2161 (1984).

[20] J.M. Baker, R.S. Rubins, *Proc. Phys. Soc.* **78,** 1353 (1961).

[21] M.L. Paradowski, A. Pacyna, A. Bombik, W. Korczak, S.Z. Korczak, *J. Magn. Magn. Mater.* **166,** 231 (1997).

[22] J.P. Sattler, J. Nemarich, *Phys. Rev. B* **4,** 1 (1971).

[23] D.J. Newman, W. Urban, *J. Phys. C* **5,** 3101 (1972).

[24] D.J. Newman, W. Urban, *Adv. Phys.* **24,** 793 (1975).

[25] A.E. Aliev, V.F. Krivorotov, P.K. Khabibullaev, *Fiz. Tverd. Tela* **39,** 1548 (1997).

[26] R. Laiho, M. Lakkisto, T. Levola, *Philos. Mag. A* **47,** 235 (1983).

[27] P. Blanchfield, G.A. Saunders, *J. Phys. C, Solid State Phys.* **12,** 4673 (1979).

[28] Y.V. Orlovskii, R.J. Reeves, R.C. Powell, T.T. Basiev, K.K. Pukhov, *Phys. Rev. B* **49,** 3821 (1994).

[29] J.M. Baker, *J. Phys. C, Solid State Phys.* **12,** 4039 (1979).

[30] H. Gerlinger, G. Schaack, *Phys. Rev. B* **33,** 7438 (1986).

[31] C. Kittel, *Introduction to Solid State Physics*, 7th ed., Wiley, New York 1996, p. 496.

[32] J.H. Van Vleck, *Phys. Rev.* **74,** 1168 (1948).

[33] M.B. Schulz, C.D. Jeffries, *Phys. Rev.* **149,** 270 (1966).